PLANT SCIENCE TODAY
ISSN 2348-1900 (online)
Vol 12(1): 1-8
https://doi.org/10.14719/pst.4867

HORIZON
e-Publishing Group
HePG

RESEARCH ARTICLE

Microcontroller-based solar tunnel dryer for sustainable drying in Northeast India

Huidrom Dayananda Singh[1], Naseeb Singh[1], Hijam Jiten Singh[1]*, Thingujam Bidyalakshmi[2], Kethavath Ajaykumar[1], Debasish Chakraborty[1] & Bira Kishore Sethy[3]

[1]Indian Council of Agricultural Research- Research Complex for North Eastern Hill Region, Umiam 793 103, Meghalaya, India

[2]Indian Council of Agricultural Research-Central Institute of Post Harvest Engineering and Technology, Ludhiana 1410 04, Punjab, India

[3]Indian Council of Agricultural Research-Indian Institute of Water Management, Bhubaneswar 751 023, Odisha, India

*Email: hijam_jiten@yahoo.co.in

OPEN ACCESS

ARTICLE HISTORY
Received: 03 September 2024
Accepted: 29 October 2024
Available online
Version 1.0 : 30 January 2025
Version 2.0 : 05 February 2025

Check for updates

Additional information
Peer review: Publisher thanks Sectional Editor and the other anonymous reviewers for their contribution to the peer review of this work.

Reprints & permissions information is available at https://horizonepublishing.com/journals/index.php/PST/open_access_policy

Publisher's Note: Horizon e-Publishing Group remains neutral with regard to jurisdictional claims in published maps and institutional affiliations.

Indexing: Plant Science Today, published by Horizon e-Publishing Group, is covered by Scopus, Web of Science, BIOSIS Previews, Clarivate Analytics, NAAS, UGC Care, etc
See https://horizonepublishing.com/journals/index.php/PST/indexing_abstracting

CITE THIS ARTICLE
Singh HD, Singh N, Singh HJ, Bidyalakshmi T, Ajaykumar K, Chakraborty D, Sethy BK. Microcontroller-based solar tunnel dryer for sustainable drying in Northeast India. Plant Science Today. 2025; 12(1): 1-8. https://doi.org/10.14719/pst.4867

Abstract

The growing world population necessitated enhanced food availability and reduced waste. Drying has been a popular technique for extending food storage for a long time since it minimizes volume and lowers moisture and enzymatic activity, reducing food loss. This project sought to create a microcontroller-driven solar tunnel dryer designed for the prevalent rainfall and elevated humidity conditions in Northeast India. The designed solar tunnel dryer is equipped with two DHT22 sensors that assess ambient humidity inside and outside the dryer, deciding whether to let airflow with the environment or isolate it. It controls fan operation based on real-time monitoring. The dryer has 12 trays on a six-tray structure that holds 100 kg of sliced turmeric in every batch. An additional tray with a load cell was provided to record turmeric weight during drying. Without any load, the maximum internal temperature exceeded the outside by 27.1°C, while the minimum internal humidity was 30% lower than external values. The turmeric was dried from an initial moisture content of 71.62% to less than 10% (wet basis) over 101 hours and 40 minutes (5 days) with 28.63 effective bright sunshine hours. The developed solar tunnel dryer's average efficiency was 19.20%, demonstrating its ability to dry turmeric in Meghalaya, India.

Keywords

humid region; microcontroller; solar tunnel dryer; turmeric

Introduction

Despite climate change, limited agricultural supplies, and land scarcity, feeding the expanding global population is a serious challenge (1). The global population is projected to exceed 9 billion by 2050, requiring a 70% increase in food availability from 2005-2007 to 2050. (2, 3). This population growth is anticipated to be concentrated in developing countries (2, 4). Food availability can be enhanced by boosting production and reducing wastage, which amounts to approximately 1.3 billion tonnes annually (3). Food losses primarily occur during consumption in developed countries, but in developing nations, losses are predominantly associated with postharvest procedures (3, 5, 6). These losses intensify food scarcity and malnutrition in low-income countries (7). Post-harvest loss in developing countries can be reduced to some extent by adopting proper drying technology.

In northeast India, turmeric and ginger are important cash crops, particularly in Meghalaya. Open sun drying is common but weather-dependent and susceptible to contamination. Alternatives such as solar tunnel dryers are feasible, but because of their performance and capacity, tunnel dryers are more practical (8). However, the rainy climate of northeast India, especially in Meghalaya, poses challenges to conventional dryers. Research has explored microcontroller-based systems to improve drying, yet these solutions are limited in capacity and often require auxiliary heating systems (9). The dried turmeric rhizome, being hygroscopic, absorbs the moisture from the humid air during the rain through the inlet and outlet. Hence, there is a need to develop microcontroller-based solar tunnel dryers that isolate themselves from the surroundings during the rainy period. It is vital to control the drying environment to maintain the product's quality and improve the system's efficiency (10). The airflow between the dryer and the surrounding environment depends on the moisture content of the air inside the dryer and the environment. In this study, an attempt has been made to develop a microcontroller-based solar tunnel dryer to isolate itself from the surroundings during the rainy period by detecting the moisture content of air inside and outside the solar tunnel dryer.

Materials and Methods

A tunnel dryer with a microcontroller was developed for drying turmeric at the Agricultural Engineering Section, Division of System Research and Engineering, ICAR Research Complex for NEH Region, Umiam, Meghalaya (25°41'18.7 "N, 91°55'06.4"E). The dryer was evaluated from November 2019 to March 2020.

Turmeric (*Curcuma longa*) harvested from the ICAR Research Complex research farms for the NEH Region, Umiam, Meghalaya, served as the study material for evaluating the developed dryer. Harvesting typically occurs from December to January in Meghalaya, with drying activities spanning from December to April. The turmeric was cleaned, washed, and boiled for 40 minutes according to the standard methodology (11). Then, the boiled turmeric was sliced into 5-8 mm thicknesses for faster drying. The turmeric slices were then placed inside the dryer, where the control system managed the drying process until reaching the desired state for grinding.

Design of tunnel dryer

The tunnel dryer (6 m x 5 m) featured an elliptical roof design with a height gradient ranging from 1.8 m to 2.8 m. Heavy mild steel square pipe (25.4 mm) was used for construction except for rafters made from mild steel flat section (30 mm × 5 mm) and enclosed with UV-treated diffused polyethene plastic sheeting (200 µm thick). The developed dryer accommodates 12 trays (measuring 1.5 m × 1.5 m) made from lightweight and corrosion-resistant aluminum sheets combined with aluminum wire mesh. Six stands inside the dryer supported the trays. The developed dryer has a capacity of 100 kg of raw, sliced turmeric per batch. Schematic representations, including a Computer-Aided Design (CAD) diagram and the physical installation, are provided in Fig. 1 and 2, respectively.

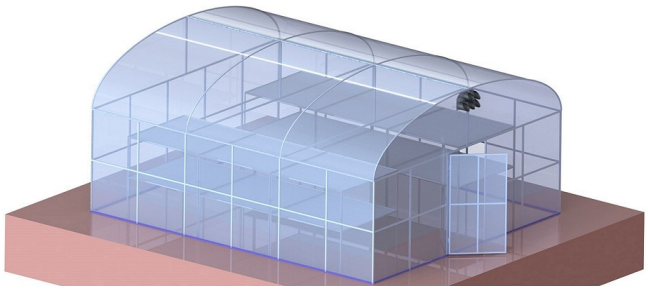

Fig. 1. CAD model of tunnel dryer.

Fig. 2. Developed tunnel dryer (Location: Engineering section, DSRE, ICAR Research Complex for NEH Region, Umiam, Meghalaya).

The movement of fresh air from the surrounding environment to the dryer and heated moist air from the dryer to the surrounding environment was controlled by an Arduino Mega 2560 with the help of DHT22 sensors, 12V DC Fans (Sunon-EEC0381B1-0000-A99), and a Nema 23 stepper motor. The system has five 10W DC fans for air exhaust and an air inlet system with a movable sliding flap operated by a Nema 23 stepper motor.

Air movement was controlled based on the difference in moisture ratio (g/m^3) calculated using temperature and relative humidity (RH) inside and outside the tunnel dryer (equations 1 to 8).

$$e_w(T) = 6.112 \times e^{\frac{17.62T}{243.12+T}} \quad \text{(Eqn.1)}$$

$$e'_w(p,T) = f(p).e_w(T) \quad \text{(Eqn.2)}$$

$$f(p) = 1.0016 + 3.15 \times 10^{-6}p - 0.074 \times p^{-1} \quad \text{(Eqn.3)}$$

$$p = p_o \times e^{\frac{-\mu g h'}{R(273+T)}} \quad \text{(Eqn.4)}$$

$$\vartheta_h = (2.83 \times 10^{-3} + 4.56 \times 10^{-3} \times H) \times (273 + T) \quad \text{(Eqn.5)}$$

$$\rho = \frac{1.0+H}{\vartheta_h} \quad \text{(Eqn.6)}$$

$$e = e_w{}' \times H \quad \text{(Eqn.7)}$$

$$X = \left(\frac{621.9907 \times e}{(p-e)}\right) \times \rho \quad \text{(Eqn.8)}$$

where,

$e_w(t)$ = saturation vapor pressure in its pure phase (hPa)

$e'_w(p,t)$= saturation vapor pressure of moist air (hPa)

e = actual vapor pressure of moist air (hPa)

p = pressure (hPa)

p_o = atmospheric pressure at mean sea level (101.325 hPa)

T = temperature (°C)

H = relative humidity (RH) in fraction

μ = molar mass of earth air (0.0289644 kg/mole)

g = gravitational acceleration (9.80665 m/s^2)

h' = height difference (994 m)

R = universal gas constant for air (8.31432 N.m/(mol.k))

X = moisture ratio (g/m^3)

An alphanumeric Liquid Crystal Display (LCD) displayed temperature, RH, moisture ratio, and the number of active fans. A cantilever-type load cell, interfaced with the microcontroller, recorded drying sample weights continuously. Real-time data, including date, time, inside and outside RH, temperature, and sample weight, were recorded every minute onto an SD card module. A 100 Wp solar panel supplied power with a 50 Ah battery and charge controller. The block diagram of the electronic system is shown in Fig. 3, and the developed control assembly in Fig. 4.

The flow chart for controlling the number of active fans and the inlet gate is depicted in Fig. 5. The dryer's system begins by checking the status of the SD card. Then, it collects temperature and humidity data inside and outside the dryer. The moisture ratios inside and outside

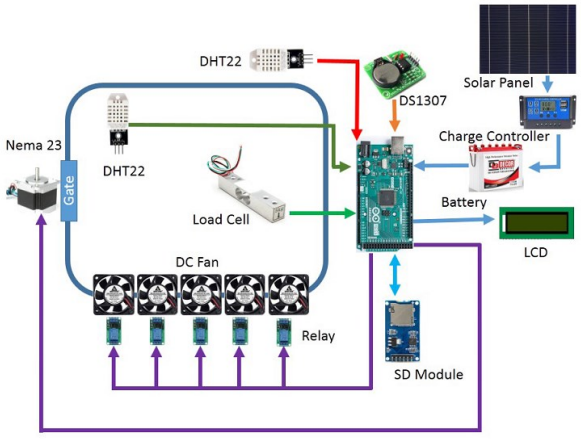

Fig. 3. Schematic diagram of the electronic system of the tunnel dryer.

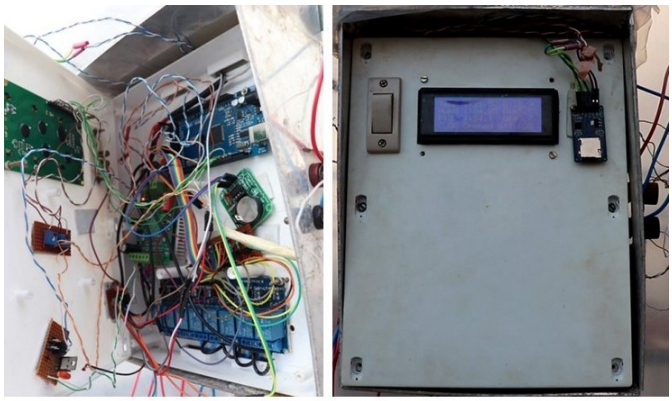

Fig. 4. Developed control system of the dryer (a) Internal view and (b) External view.

the dryer are calculated using this data. If the inside temperature exceeds 55°C, the number of active fans is adjusted by increasing or decreasing it by one based on the previous inside temperature. When indoor humidity reaches 95% or exceeds it, and outdoor humidity is below 98%, all five fans are engaged to evacuate the humid air from the inside.

On the other hand, no fans will run, and the inlet gate will be closed to restrict the entry of moist outside air if the outside humidity is 98% or higher. Furthermore, the number of active fans will be raised if the difference in moisture ratio between the inside and outside of the dryer is greater than before. The number of active fans will be reduced if the moisture ratio difference is less than the one before.

Measurement of parameters

Solar insolation at the study site was measured using a pyranometer (Apogee SP-420), set horizontally on the same plane as the dryer. Readings were taken at 15-second intervals and averaged every 15 minutes. DHT22 sensors were utilized for temperature and relative humidity (RH) measurements. One DHT22 was placed at the center of the tunnel dryer to measure average inside temperature and RH as there is minimal temperature variance within the dryer, and lower RH levels were revealed at the inlet and higher levels at the outlet (12). At the same time, another was positioned outside within a sheltered structure to prevent direct sunlight exposure. A digital load cell (10 kg capacity) and the HX711 module monitored the sample weight within the tunnel dryer. The sample weight was recorded at minute intervals, with the load cell positioned beneath a tray measuring 0.5 m × 0.4 m.

Performance evaluation

The system's performance was evaluated based on drying time and drying efficiency by using equations. 9 to 12.

$$m_d = \frac{W-W_s}{W_s} \quad \text{(Eqn.9)}$$

$$m_w = \frac{W-W_s}{W} \quad \text{(Eqn.10)}$$

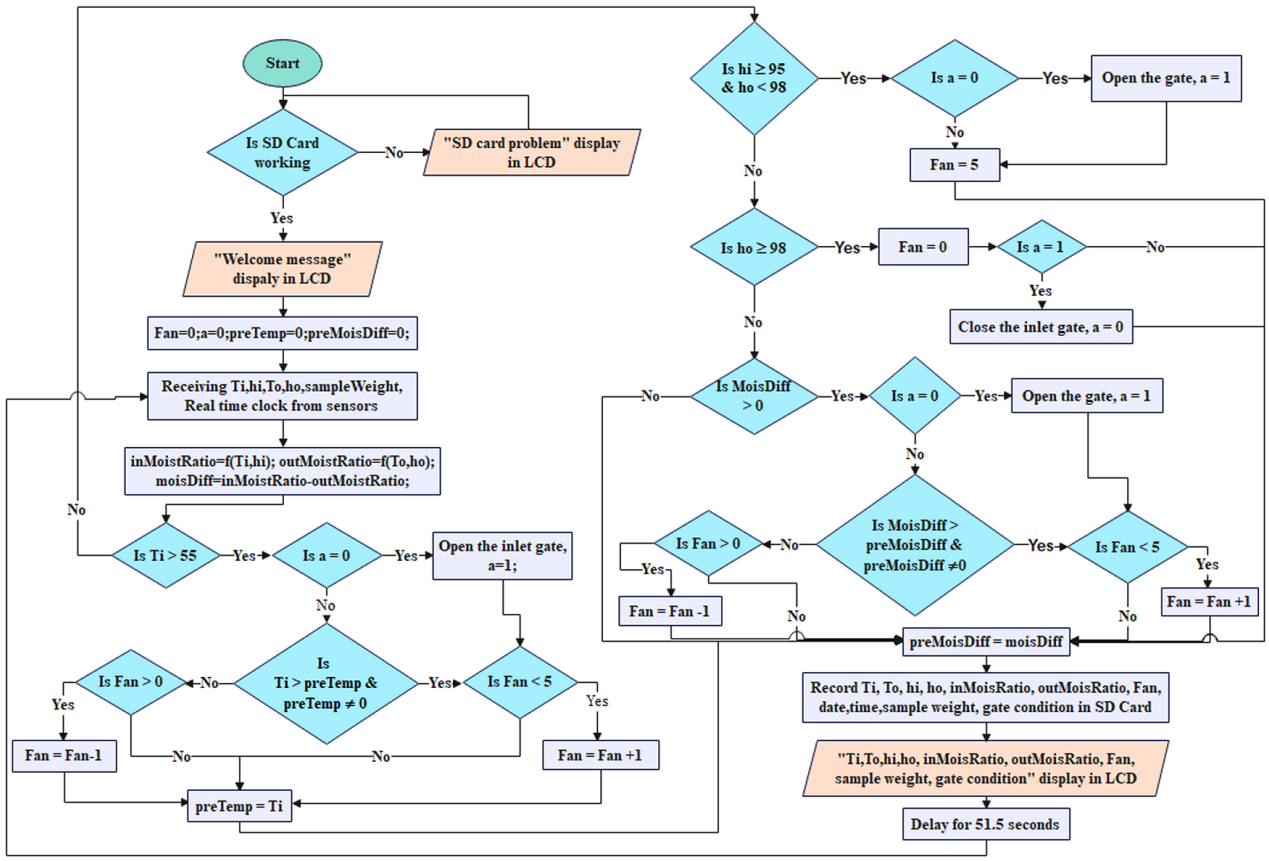

Fig. 5. Flowchart for operation of fan and inlet gate of the dryer for controlling drying environment.

$$F_h = \sum_i^n F_i \times t_i \quad \text{(Eqn.11)}$$

$$Efficiency = \frac{m_{we} \times \theta_w}{(I \times A \times t) + (\sum_{i=1}^{15} (n_{if} \times p_f \times 60) + (p_s \times t)} \quad \text{(Eqn.12)}$$

where,

W = Initial weight of the sample, g.

W_s = Oven-dried weight of the sample, g.

m_d = moisture content (dry basis)

m_w = moisture content (wet basis)

F_h = Active fan in a day, fan-hour.

F_i = Numbers of fans active in a particular duration.

t_i = duration in which Fi fans are active, h.

m_{we} = water evaporates, kg.

θ_w = latent heat of water, kJ/kg.

I = solar radiation received inside the dryer through the polyethene plastic sheet, w/m^2.

A = net surface area of the greenhouse dryer, m^2.

n_f = number of active fans.

p_f = power consumption of a fan, W.

p_s = power consumption by system excluding fan, W.

t = time, s.

Drying during the effective bright sunshine (more than or equal to 120 W/m^2) was considered for efficiency calculation (13). The efficiencies were reported hourly to smoothen the variation to some extent. An equal weight of turmeric per unit tray surface area was loaded onto each tray, including the sample tray, to ensure uniformity. The samples dried on the tray with the load cell inside the tunnel dryer were kept in an electric oven at 60°C for 48 hours to determine the final moisture content (14). This final bone-dry weight was used to determine the moisture content of the turmeric samples during the drying period.

Results and Discussion

The higher humidity at the research site creates difficulty in maintaining a drying environment. In this situation, a microcontroller-based solar tunnel dryer offered a distinct advantage by continuously monitoring the dryer's inside and outside temperature and humidity and controlling the drying process by comparing internal and external air moisture content (15). Based on this comparison, this control mechanism enabled decisions to sustain or halt drying. Evaluation of the dryer's efficacy focused on two main parameters: time to reach desired moisture content in turmeric and overall drying efficiency.

Fig. 6a and Fig. 6b represents the fluctuations observed in temperature and RH levels inside and outside the tunnel dryer without any loaded samples. It was observed that the maximum inside temperature exceeded the outside temperature by 27.10°C, while the minimum

inside RH was 30% lower than the external RH, which corroborated an earlier report (16).

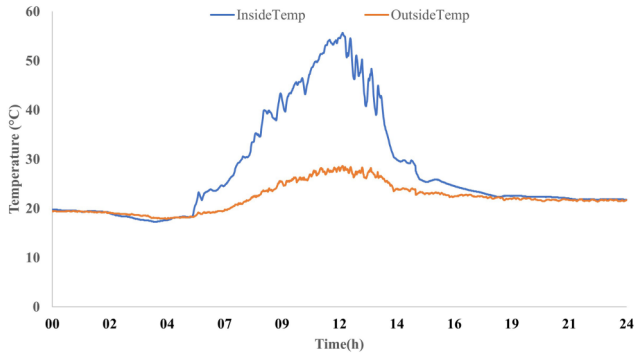

Fig. 6 (a). Temperature and humidity at no load condition temperature.

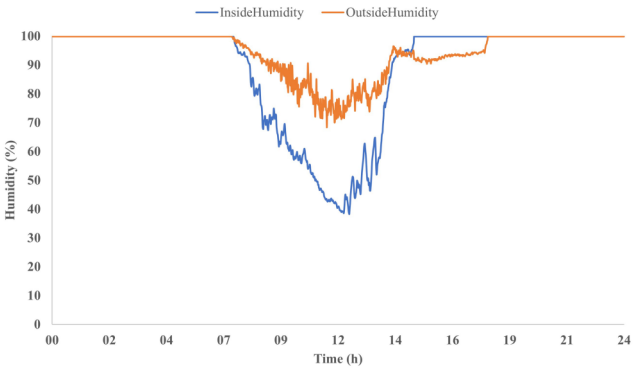

Fig. 6 (b). Temperature and humidity at no load condition humidity.

The load test involved drying sliced turmeric (5 to 8 mm) and weighing 100 kg after blanching. The initial moisture content of the turmeric was determined using eqn. (10) and was found to be 71.62% on a wet basis (w.b.). Fig. 7 and Fig. 8, respectively, displayed the fresh turmeric's appearance before drying and the dried turmeric within the tunnel dryer.

Fig. 7. Fresh turmeric inside the tunnel dryer.

Fig. 8. Dried turmeric inside the tunnel dryer (cumulative time: 97:03 h, day: 5th, inside temperature: 32.6°C, inside humidity: 50.6%, outside temperature: 22.5°C, outside humidity: 58.6%, sunshine intensity: 255 W).

The turmeric samples were dried in the tunnel dryer for 101 hours and 40 minutes (5 days). Fluctuations in temperature and RH inside and outside the dryer, along with sunshine data, are illustrated in Fig. 9-11. The graphical representation shows the progression over each day, with distinct segments delineating each day's data (Y-axis-A: Day 1, A-B: Day 2, B-C: Day 3, C-D: Day 4, and After D: Day 5).

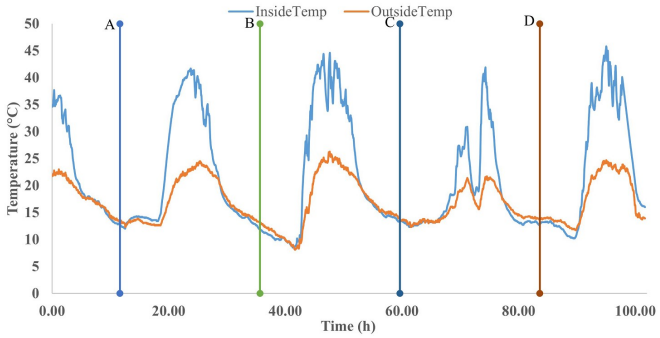

Fig. 9. Temperature inside and outside of tunnel dryer (h – hour).

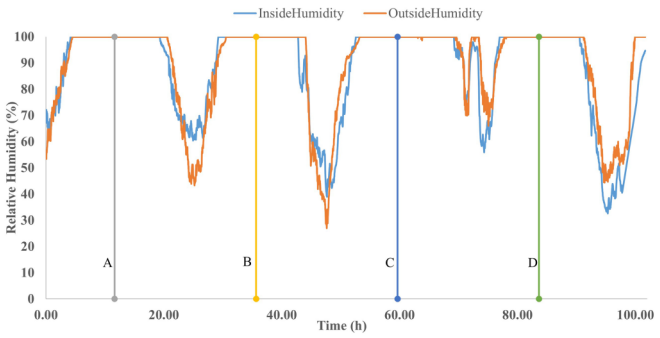

Fig. 10. Humidity inside and outside of the tunnel dryer (h – hour).

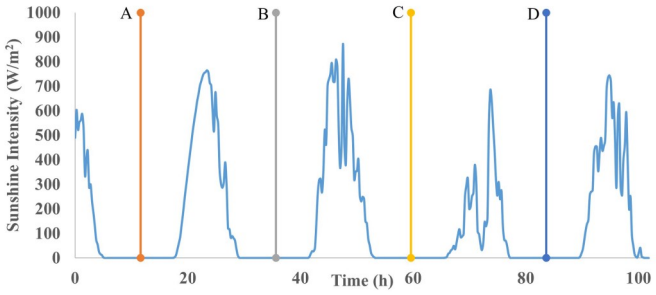

Fig. 11. Solar intensity (h – hour).

The maximum inside temperatures of the dryer on the first, second, third, fourth, and fifth days were recorded as 37.70°C, 41.70°C, 44.60°C, 41.90°C, and 45.80° C, respectively, against outside maximum temperatures of 23.00°C, 24.50°C, 26.30°C, 21.70°C, and 24.70°C for the corresponding days. A study reported a maximum drying temperature of 45.70°C during coffee bean drying in a solar dryer (17). During the early drying stages, the inside RH was higher than the outside RH. However, as the drying progressed, the inside RH gradually decreased below the outside RH. This phenomenon may be attributed to the decreasing moisture level in the turmeric samples, hence lowering the moisture content of the air within the dryer. The observed pattern indicated that with the advancement of the drying process, inside temperatures escalated while inside RH declined. Chavan et al. mentioned a similar pattern of increasing temperature

and decreasing RH inside the dryer as the drying progresses while drying fish in a solar cabinet dryer (18).

Fig. 12 illustrates the fluctuation in active fans throughout the drying period, concurrently displaying the corresponding solar intensity variation each day. The operations of the dryer's fans were active mainly in the morning when solar intensity exceeded 300 W/m^2. A delay in drying activity after sunrise may be attributed to the time needed to build up temperature following solar radiation receipt. Initially, on the first and second days, nearly all five fans were active throughout most of the daytime, but as drying progressed, fluctuations in the number of active fans increased. This variation may result from decreased moisture content in the inside air during drying, leading to a reduced moisture content difference between the inside and outside air. The number of operating fans dropped to zero when this difference was close to zero or when the moisture content of the outside air was higher than the temperature inside. On the other hand, there may occasionally be five active fans in the evening when solar intensity drops. This response was governed by the control system algorithm, instructing rapid removal of humid air when temperature decreased to prevent moisture condensation on the dryer's internal surface.

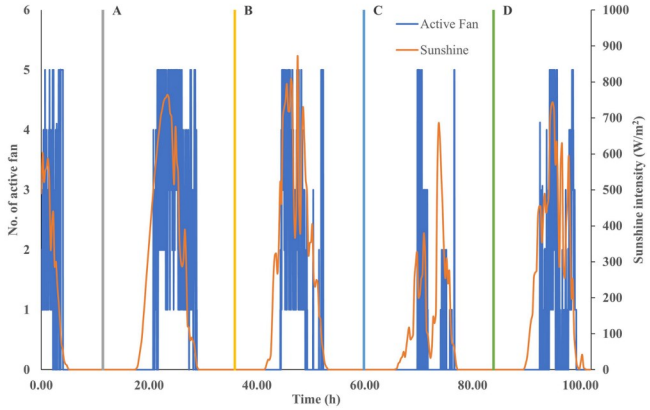

Fig. 12. Active fan during drying period along with the sunshine intensity (h – hour).

On the fourth day, there were no active fans around noon, likely due to recorded precipitation of 0.8 mm at the drying site (weather station at ICAR, Umiam). During such periods, the developed control system isolated the dryer from the surrounding environment by closing the inlet gate with no active fan operation. Drying resumed once the surrounding environment became favorable. Fig. 13 depicts the duration of active fan operation throughout the drying process.

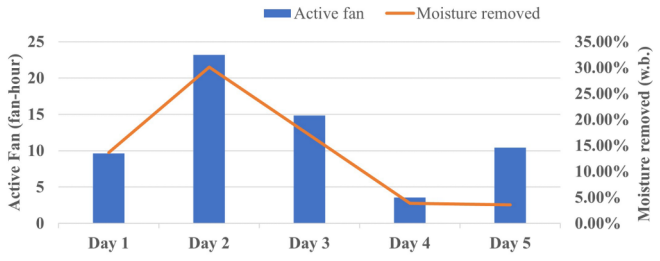

Fig. 13. The active fan time along with the moisture dried on that day (h – hour).

On the first day, fan operation was brief due to late material introduction, limiting drying time and moisture removal. On the other hand, there was more fan operation and moisture removal on the second day. However, both parameters decreased on the third day due to diminishing moisture release from the turmeric. The minimal fan operation on the fourth day was attributed to reduced solar radiation, as shown in Fig. 12. Lastly. However, fan duration increased on the fifth day, and moisture removal did not proportionally increase due to the heightened energy demand for drying as the process progressed.

Drying curve

The drying process is visualized in a drying curve, illustrating moisture content changes over time (Fig. 14). Initially, moisture decreased from 71.62% to 57.99% between 12:20 Hours and 19:17 Hours on the first day and further to 57.15% by 06:47 hours on the second day. Drying continued to reduce moisture from 57.15% to 27.04% between 06:47 hours and 16:56 Hours on the second day. A similar trend occurred during the second night, decreasing to 26.44% by 06:59 Hours on the third day.

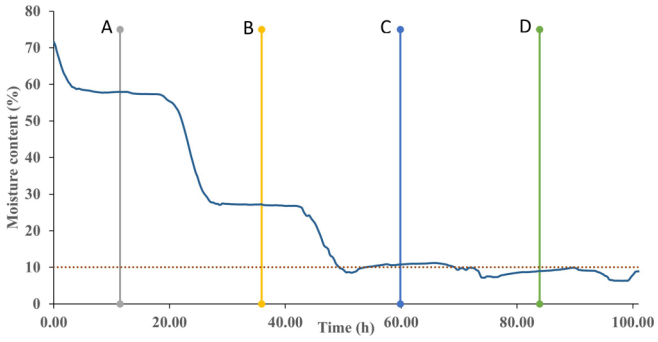

Fig. 14. Drying curve of turmeric (h – hour).

Drying progressed from 26.44% to 9.44% on the third day between 06:59 and 16:55 hrs. However, moisture absorption was observed during the third night, increasing to 11.15% by 06:26 Hours on the fourth day. Drying reduced moisture from 11.15% to 7.29% by 16:24 hours on the fourth day. During the fourth night, moisture was absorbed again, reaching 9.86% by 05:59 hours on the fifth day. Subsequently, drying resumed until 15:59 Hours, reducing moisture to 6.31%. The turmeric absorbed moisture again and reached 8.98% by 18:02 hours. Thus, the developed dryer achieved the desired moisture content (less than 10%) in five drying days (101 hours and 40 minutes). A study revealed that turmeric achieved the requisite moisture content of 10% in 64 hours using a natural convection dryer, whereas sun drying required 96 hours to attain the same moisture level (19). Using whole turmeric and natural draft dryers in their work may need more time to dry in their dryer.

Efficiency

The efficiency of the microcontroller-based solar tunnel dryer was calculated using Eqn. 12, along with the parameters in Table 1. The hourly average efficiency of the dryer during the drying period is given in Fig. 15.

The dryer's efficiency varied from 35.14% to 2.10%, averaging 19.20%. Achieving the target moisture content

Table 1. Constants used in the calculation of efficiencies

Sl. No.	Parameter	Value
1	latent heat of water (θ_w)	2260 kJ/kg
2	The net surface area of the tunnel dryer (A)	30 m^2

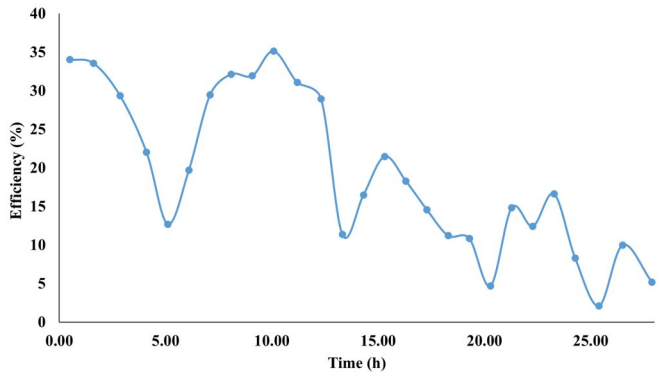

Fig. 15. The efficiencies of the dryer during the drying period (h – hour).

of less than 10% (w.b.) required 28.63 effective hours of bright sunshine. Efficiency was initially higher and decreased as drying progressed, likely due to the increased energy needed to remove water at lower moisture levels. Efficiency increases when radiation decreases, possibly due to thermal energy released from materials inside the dryer. A similar variation in efficiency was reported while working with solar greenhouse dryers (20). The overall efficiency of the solar tunnel dryer developed in a study was reported as 17.9% with pomegranate samples (21). The thermal efficiency of the greenhouse dryer was evaluated with an onion slice after pre-treatment, and it was found to be 20.82% (22). A cabinet-type solar dryer with a 5 kg capacity is reported to have a higher % drying efficiency of 27% while drying ginger (23).

Conclusion

The microcontroller-based solar tunnel drier, utilizing DHT22 sensors for internal and external data, demonstrated notable temperature and humidity differentials between its inside and the external environment. During no-load tests, it maintained a maximum temperature difference of 27.10°C higher inside than outside, alongside a 30% lower relative humidity. Throughout the five-day drying process with a 100 kg turmeric load, the dryer effectively reduced the turmeric's initial moisture content from 71.62% to less than 10% (w.b.) using 28.63 effective bright sunshine hours. Despite fluctuations, the dryer's efficiency ranged from 35.14% to 2.10%, with an average of 19.20%, demonstrating its effectiveness in drying turmeric. Future improvements may involve integrating additional heating systems for continuous drying, especially during nighttime and cloudy periods, thereby reducing overall crop drying time.

Acknowledgments

The Authors acknowledge the financial support of the All India Coordinated Research Project on Plastic Engineering in Agriculture Structure and Environment Management for carrying out the research work. The authors also acknowledge the support the Director of ICAR Research Complex provided for NEH Region, Umiam, Meghalaya.

Author's Contribution

HDS, NS, HJS, TB, and BKS conceptualized, designed, and developed the tunnel dryer. HDS, NS, DC, and BKS evaluated this dryer. HDS, TB, and KA analyzed the data. HJS and HDS assembled the initial draft of the manuscript. All authors reviewed, commented on, and edited subsequent versions. All authors approved the final manuscript after a thorough review.

Conflict of interest: Authors do not have any conflict of interest to declare.

Ethical issues: None

References

1. Bradford KJ, Dahal P, Van Asbrouck J, Kunusoth K, Bello P, Thompson J, et al. The dry chain: Reducing postharvest losses and improving food safety in humid climates. Trends Food Sci Technol. 2018;71:84-93. https://doi.org/10.1016/j.tifs.2017.11.002
2. Food and Agriculture Organization of the United Nations. How to feed the world in 2050. Rome: Food and Agriculture Organization of the United Nations; 2009 [cited 2023 Nov 13]. 35 p. Available from: https://www.fao.org/fileadmin/templates/wsfs/docs/expert_paper/How_to_Feed_the_World_in_2050.pdf
3. Food and Agriculture Organization of the United Nations. The state of food insecurity in the world: How does international price volatility affect domestic economies and food security? Rome: Food and Agriculture Organization of the United Nations; 2011 [cited 2023 Nov 13]. 55 p. Available from: https://www.uncclearn.org/wp-content/uploads/library/fao_food_insecurity.pdf
4. Udomkun P, Romuli S, Schock S, Mahayothee B, Sartas M, Wossen T, et al. Review of solar dryers for agricultural products in Asia and Africa: An innovation landscape approach. J Environ Manag.2020;268:110730. https://doi.org/10.1016/j.jenvman.2020.110730
5. Chegere MJ. Post-harvest losses reduction by small-scale maize farmers: The role of handling practices. Food Policy. 2018;77:103-15. https://doi.org/10.1016/j.foodpol.2018.05.001
6. Hodges RJ, Buzby JC, Bennett B. Postharvest losses and waste in developed and less developed countries: Opportunities to improve resource use. J Agric Sci. 2011;149(S1):37-45. https://doi.org/10.1017/S0021859610000936
7. Food and Agriculture Organization of the United Nations. The state of food insecurity in the world: Addressing food insecurity in protracted crises. Rome: Food and Agriculture Organization of the United Nations; 2010 [cited 2023 Nov 13]. 62 p. Available from: https://www.fao.org/4/i1683e/i1683e.pdf
8. Sacilik K, Keskin R, Elicin AK. Mathematical modelling of solar tunnel drying of thin layer organic tomato. J Food Eng. 2006;73(3):231-38. https://doi.org/10.1016/j.jfoodeng.2005.01.025
9. Jibia AU, Umar S. Microcontroller-based fruit drying system. ATBU J Sci Technol Educ. 2015;3(3):102-10.
10. Devi TB, Kalnar YB. Design consideration of smart solar dryer for precision drying: Smart solar dryer for precision drying. J AgriSearch. 2021;8(2):135-38.

11. Jayashree E, Zachariah TJ. Processing of turmeric (*Curcuma longa*) by different curing methods and its effect on quality. Indian J Agric Sci. 2016;86(5):696-98. https://doi.org/10.56093/ijas.v86i5.58358
12. Kaewkiew J, Nabnean S, Janjai S. Experimental investigation of the performance of a large-scale greenhouse type solar dryer for drying chilli in Thailand. Procedia Eng. 2012;32:433-39. https://doi.org/10.1016/j.proeng.2012.01.1290
13. World Meteorological Organization (WMO). Manual on the Global Observing System. Volume I (Annex V to the WMO Technical Regulations) [Internet]. WMO-No. 544. 2010 [cited 2023 Oct 20]. Available from: https://www.met.gov.fj/icao/volI.pdf
14. Venkateshwari T, Ganapathy S, Arulmari R, Vijayakumary P. Effect of drying temperature on the curcumin content of turmeric rhizomes (*Curcuma longa* L.). Pharma Innovation. 2021;10(10):2349-51.
15. Department of Agriculture Meghalaya. Meghalaya agriculture profile [Internet]. 3rd ed. Meghalaya: Department of Agriculture Meghalaya; 2006 [cited 2023 Oct 7]. Available from: https://www.megagriculture.gov.in/PUBLIC/dwd_docs/MegAgriProfile2006.pdf
16. Mkhathini KM, Magwaza LS, Workneh TS, Mwithiga G. Effects of relative humidity and temperature on small scale peach fruit drying using a tunnel solar dryer: A case study of peach fruit produced by small scale farmers in the Midlands of Kwazulu-Natal, South Africa. S Afr J Agric Ext. 2018;46(2):1-13. http://dx.doi.org/10.17159/2413-3221/2018/v46n2a454.
17. Mengesha TT. Performance evaluation of forced convection solar dryer under Jimma condition. International Journal of Scientific and Research Publications. 2020;10(06):264-76. https://doi.org/10.29322/IJSRP.10.06.2020.P10232
18. Chavan BR, Yakupitiyage A, Kumar S. Mathematical modeling of drying characteristics of Indian mackerel (*Rastrilliger kangurta*) in solar-biomass hybrid cabinet dryer. Dry Technol. 2008;26(12):1552-62. https://doi.org/10.1080/07373930802466872
19. Gunasekar JJ, Kaleemullah S, Doraisamy P, Kamaraj S. Evaluation of solar drying for postharvest curing of turmeric (*Curcuma longa* L.). AMA Agric Mech Asia Afr Lat Am. 2006;37(1):9-13.
20. Condorí M, Echazú R, Saravia L. Solar drying of sweet pepper and garlic using the tunnel greenhouse drier. Renew Energy. 2001;22(4):447-60. https://doi.org/10.1016/S0960-1481(00)00098-7
21. Kumar M, Mahore A, Choudhary MK, Lalita, Nalawade R, Patel A, et al. Development of mini solar tunnel dryer and validation of thin layer drying models for pomegranate seeds. Int J Environ Clim Change. 2023;13(2):42-49. https://doi.org/10.9734/IJECC/2023/v13i21651
22. Dattatreya MK, Nangare DD, Singh R, Kumar S. Low-cost greenhouse technology for drying onion (*Allium cepa* L.) slices. J Food Process Eng. 2011;34(1):67-82. https://doi.org/10.1111/j.1745-4530.2008.00337.x
23. Devi TB, Singh SK, Mani I, Kumar S, Yadav V, Singh Y, et al. Solar dryer using evacuated tube solar thermal collector with thermal storage. Indian J Agri Sci. 2023;93(2):233-36. https://doi.org/10.56093/ijas.v93i2.109915